Comparing Multitarget Multisensor ML-PMHT with ML-PDA for VLO Targets

Steven Schoenecker
NUWC
Division Newport
Newport, RI
Email: steven.schoenecker@navy.mil

Peter Willett
Electrical Engineering
University of Connecticut
Storrs, CT
Email: willett@engr.uconn.edu

Yaakov Bar-Shalom
Electrical Engineering
University of Connecticut
Storrs, CT
Email: ybs@engr.uconn.edu

***Abstract*—The Maximum Likelihood Probabilistic Data Association (ML-PDA) tracker and the Maximum Likelihood Probabilistic Multi-Hypothesis (ML-PMHT) tracker are tested in their capacity as algorithms for very low observable targets (VLO, meaning 6 dB post-signal-processing or even less) and are then applied to five synthetic benchmark multistatic active sonar scenarios featuring multiple targets, multiple sources and multiple receivers. Both methods end up performing well in situations where there is a single target or widely-spaced targets. However, ML-PMHT has an inherent advantage over ML-PDA in that its likelihood ratio has a simple multitarget formulation, which allows it to be implemented as a true multitarget tracker. This formulation gives ML-PMHT superior performance for instances where multiple targets are closely spaced with similar motion dynamics.**

Keywords: ML-PDA, ML-PMHT, multitarget ML-PMHT, maximum likelihood, multistatic, bistatic, sonar, tracking, multitarget, very low observable.

I. Introduction

The Maximum Likelihood Probabilistic Data Association (ML-PDA) tracker and the Maximum Likelihood Probabilistic Multi-Hypothesis (ML-PMHT) tracker are both algorithms that can be used in an active multistatic sonar framework. With some basic assumptions about a target (or targets) as well as the environment, likelihood ratios can be developed for both algorithms and then maximized to obtain target motion parameter estimates. The main difference between the two algorithms is in the measurement-to-target assignment model; ML-PDA assumes that at most one measurement per scan can originate from a target, while ML-PMHT allows for any number of measurements to have originated from a target. While this assumption may reduce the appeal of ML-PMHT to some, the resulting algorithm does offer a significant advantage in terms of its multitarget formulation.

The concept behind ML-PDA was first introduced in [4], while the ideas behind ML-PMHT originated in [2], [9], [10], and [11]. The assumptions used to develop the ML-PDA and ML-PMHT algorithms are covered in detail in [8]; we merely summarize the results here. This work began in [6], which implemented both ML-PDA and ML-PMHT as sequential single-target trackers. In [8], ML-PMHT was for the first time implemented as a true multitarget tracker. This paper is a condensed version of that work. The ML-PDA log-likelihood ratio (LLR) for a batch of data is

$$\Lambda(\mathbf{x}, Z) = \sum_{i=1}^{N_w} \ln \left\{ 1 - P_d + \frac{P_d}{\lambda} \sum_{j=1}^{m_i} p[\mathbf{z}_j(i)|\mathbf{x}] \rho_j(i) \right\} \quad (1)$$

where P_d is the target probability of detection in a scan, λ is the spatial clutter density, N_w is the number of scans, m_i is the number of measurements in the i^{th} scan, $\mathbf{z}_j(i)$ is the j^{th} measurement in the i^{th} scan, $p[\mathbf{z}_j(i)|\mathbf{x}]$ is a target-centered Gaussian, $\rho_j(i)$ is the amplitude likelihood ratio, $\mathbf{x}$ is the target state motion parameter[1], and Z is the (entire) set of measurements in the batch. The ML-PMHT LLR is given by

$$\Lambda'(\mathbf{x}, Z) = \sum_{i=1}^{N_w} \sum_{j=1}^{m_i} \ln \left\{ \pi_0 + \pi_1 V p[\mathbf{z}_j(i)|\mathbf{x}] \rho_j(i) \right\} \quad (2)$$

where π_0 is the prior probability that a measurement is from clutter, π_1 is the prior probability that a measurement is from the target, and V is the search volume in the measurement space. The ML-PMHT algorithm has an advantage over ML-PDA in that its LLR can be expressed naturally in multitarget form. This is given as

$$\Lambda^{\dagger}(\mathbf{x}, Z) = \sum_{i=1}^{N_w} \sum_{j=1}^{m_i} \ln \left\{ \pi_0 + V \sum_{k=1}^{K} \pi_k p[\mathbf{z}_j(i)|\mathbf{x}_k] \rho_{jk}(i) \right\} \quad (3)$$

where π_k is the probability that a given measurement is from the k^{th} target and $\sum_{k=0}^{K} \pi_k = 1$.

Additionally in [8], an expression was developed for the Cramér-Rao Lower Bound (CRLB) for ML-PMHT, and it was shown that the ML-PMHT estimator is efficient, so the CRLB can be used to represent the covariance $\mathbf{C}$ of the estimated target parameter vector. This CRLB is computed by first calculating the Fisher Information Matrix (FIM) $\mathbf{J}_i$ for a single data scan

$$\mathbf{J}_i = \mathbf{D}_{\phi}^T \sum_{j=1}^{m_i} \mathbf{G}_j^T \int_V \frac{\frac{[\pi_1 p_1^{\tau}(a_j)]^2}{|2\pi \mathbf{R}_j|} e^{-\xi_j^T \xi_j} \xi_j \xi_j^T}{\frac{\pi_0 p_0^{\tau}(a_j)}{V} + \frac{\pi_1 p_1^{\tau}(a_j)}{\sqrt{|2\pi \mathbf{R}_j|}} e^{-\frac{1}{2}\xi_j^T \xi_j}} \times d\xi_j da_j \frac{\mathbf{G}_j}{|\mathbf{G}_j|} \mathbf{D}_{\phi} \quad (4)$$

Supported by ONR grants N00014-10-10412, N00014-10-1-0029, N00014-13-1-0231, and ARO grants W911NF-06-1-0467 and W911NF-10-1-0369.
Proc. 16th Intn'l Conf. Info. Fusion. Istanbul, Turkey, July 2013.

[1]The target motion is assumed to be described by the parameter $\mathbf{x}$, i.e. it is modeled as noiseless (without process noise) in the window of N_w scans.

Report Documentation Page

Form Approved
OMB No. 0704-0188

1. REPORT DATE	2. REPORT TYPE	3. DATES COVERED
JUL 2013		**00-00-2013 to 00-00-2013**

4. TITLE AND SUBTITLE	5a. CONTRACT NUMBER
Comparing Multitarget Multisensor ML-PMHT with ML-PDA for VLO Targets	5b. GRANT NUMBER
	5c. PROGRAM ELEMENT NUMBER
6. AUTHOR(S)	5d. PROJECT NUMBER
	5e. TASK NUMBER
	5f. WORK UNIT NUMBER
7. PERFORMING ORGANIZATION NAME(S) AND ADDRESS(ES) **Naval Undersea Warfare Center,Division Newport,Newport,RI,02841**	8. PERFORMING ORGANIZATION REPORT NUMBER
9. SPONSORING/MONITORING AGENCY NAME(S) AND ADDRESS(ES)	10. SPONSOR/MONITOR'S ACRONYM(S)
	11. SPONSOR/MONITOR'S REPORT NUMBER(S)

12. DISTRIBUTION/AVAILABILITY STATEMENT
Approved for public release; distribution unlimited

13. SUPPLEMENTARY NOTES
Presented at the 16th International Conference on Information Fusion held in Istanbul, Turkey on 9-12 July 2013. Sponsored in part by Office of Naval Research Global.

14. ABSTRACT
The Maximum Likelihood Probabilistic Data Association (ML-PDA) tracker and the Maximum Likelihood Probabilistic Multi-Hypothesis (ML-PMHT) tracker are tested in their capacity as algorithms for very low observable targets (VLO meaning 6 dB post-signal-processing or even less) and are then applied to five synthetic benchmark multistatic active sonar scenarios featuring multiple targets, multiple sources and multiple receivers. Both methods end up performing well in situations where there is a single target or widely-spaced targets. However ML-PMHT has an inherent advantage over ML-PDA in that its likelihood ratio has a simple multitarget formulation, which allows it to be implemented as a true multitarget tracker. This formulation gives ML-PMHT superior performance for instances where multiple targets are closely spaced with similar motion dynamics.

15. SUBJECT TERMS

16. SECURITY CLASSIFICATION OF:			17. LIMITATION OF ABSTRACT	18. NUMBER OF PAGES	19a. NAME OF RESPONSIBLE PERSON
a REPORT **unclassified**	b ABSTRACT **unclassified**	c THIS PAGE **unclassified**	**Same as Report (SAR)**	**8**	

where $\mathbf{D}_\phi$ is the Jacobian of the measurement function ϕ with respect to the parameter $\mathbf{x}$, $\mathbf{R}_j$ is the measurement noise covariance for the j^{th} measurement, and $\mathbf{G}_j$ is the Cholesky factor of $\mathbf{R}_j^{-1}$. Finally, p_1^τ and p_0^τ are the amplitude likelihoods for the target and clutter, respectively. The FIM for a batch of data is simply the sum of the FIMs for each scan in the batch, and then the CRLB covariance $\mathbf{C}$ is just the inverse of the batch FIM.

The ML-PDA LLR in (1) is for a single target only. In order to make this algorithm function as a multi-target tracker, it is necessary to implement it in a sequential single-target mode. This is done by maximizing the LLR for a batch of data. If this LLR at the optimum point exceeds a certain threshold, a track is declared. Next, the measurement in each scan that has the greatest probability of being associated with the target is excised from the data. The LLR is then maximized again on the new batch of data, and the process is repeated until no more tracks can be found. This approach worked reasonably well for multiple targets in past work [7].

In contrast, ML-PMHT has a natural multitarget formulation (3). The ML-PMHT multitarget tracking framework was implemented in two steps. The first was the single track extraction sequence and testing all extracted tracks for "closeness." In the second step, any tracks that were determined to be close were grouped together and optimized with the multitarget ML-PMHT log-likelihood ratio formulation in (3). Grouping tracks involved estimating the state covariance of all existing tracks. We let the CRLB shown above represent the state covariance $\mathbf{C}_n$ for the n^{th} target, and with this, a χ^2 test statistic [3] is evaluated for closeness between all possible pairs of active tracks in the form

$$S_{mn} = \Delta\hat{\mathbf{x}}_{mn}^T(\mathbf{C}_m + \mathbf{C}_n)^{-1}\Delta\hat{\mathbf{x}}_{mn} \tag{5}$$

where $\Delta\hat{\mathbf{x}}_{mn} = \hat{\mathbf{x}}_m - \hat{\mathbf{x}}_n$ (the difference of the parameter vector estimates between the m^{th} and n^{th} track). All track pairs with a statistic S_{mn} less than a given threshold are grouped together. More than two tracks could belong to a group by the use of this association — to join a group, an ungrouped track only had to meet the test described in (5) with one of the tracks already in the group.

II. Simulation Descriptions

Five benchmark multistatic sonar scenarios, initially developed in [6], were used to measure performance differences between ML-PDA and ML-PMHT with Monte Carlo testing. Each scenario was designed so target detections from a single source-receiver pair would be present approximately 80 percent of the time in a given scan, and clutter was set at a level that made the problem as difficult as possible while not slowing down run times to the point of precluding Monte Carlo testing. The clutter amplitude in the five scenarios was given a K-distribution [1]. Scenario 1 was also run with Rayleigh-distributed clutter [5] in a relatively high-clutter environment. The various scenario parameters are listed in Table I (these parameters, used in the simulation, were also matched in the actual ML-PDA and ML-PMHT tracking code). All scenarios are shown in Figures 3–14. (For clarity, we note that this sequence of figures is used both in this section to illustrate the geometries used and in Section III to provide examples of individual results.) Each of the scenario target geometries was designed for a specific test purpose. Then, given these target geometries, the sensors were laid out in an effort to obtain an average target P_d of 0.8 in any given scan. (The one exception to this occurs in Scenario 5 and is described below.) The pinging strategy was purposely kept very simple — every transmitter had a (simulated) ping every 60 seconds. The scenarios are described as follows:

1) Baseline Scenario: Scenario 1, shown in Figure 3, featured a single target moving in a straight line past a source and a receiver (the source was a receiver as well). This was intentionally created as one of the simplest possible multistatic scenarios. In theory, ML-PDA and ML-PMHT should converge to the same value under benign conditions (this is shown in detail in [8]), and this scenario is a case where this convergence should hold true.

2) Close Targets with Similar Dynamics Scenario: Scenario 2, shown in Figure 5, features three targets very close together (they have a separation of only 500 distance units) with similar motion dynamics – i.e. they are maneuvering in a coordinated fashion. This makes it very difficult for any algorithm to distinguish and separate targets from each other. This will test if the multitarget implementation for ML-PMHT is an improvement over the sequential single-target implementation of ML-PDA.

3) Close Targets with Different Dynamics Scenario: Scenario 3, shown in Figure 7, has two targets closing each other from the east and west. During the middle of the scenario, the targets will be in close proximity to each other, but they will have different motion dynamics — at the time they are close, they will be moving in opposite directions. (Although the targets have the same course after the right-hand target's course change, they are not close to each other after the maneuver.) Again, this is designed to test each tracker's ability to follow close targets, but under slightly easier circumstances than in scenario 2.

4) Large Number of Targets Scenario: Scenario 4, shown in Figure 9, features ten very low-speed targets and three relatively high-speed targets. This scenario was designed simply to measure each algorithm's ability to track a (relatively) large number of targets, especially when some of those targets are low-speed and exhibit very low Doppler.

5) Switching Targets Scenario: Scenario 5, shown in Figure 11, is similar to scenario 2 in that it has two targets in close proximity to each other with the same motion dynamics. However, the targets start out with a distinct separation and then close on each other. At the point where the targets are about to intersect, they turn and parallel each other. Such motion, with the targets approaching each other (where their projected motion has them crossing), will make it very difficult for any trackers continually to associate measurements with the correct targets and not to switch targets. Additionally, this scenario was given a relatively high number of receivers (16), and due to the geometry, most source receiver pairs will have a P_d of much less than 0.8 — many scans will just have clutter measurements. This is effectively raising the clutter levels that the tracker will see.

These scenarios were all run using the ML-PDA target measurement generation model, where the target produced at most one measurement per scan. Scenario 1 was then

re-run with the ML-PMHT target measurement generation model, where more than one measurement was allowed to be generated by the target in a scan. This scenario was run three separate times with the expected number of target measurements per scan set at one, two and three, respectively. (Note the case of one target measurement per scan is not the ML-PDA target measurement generation model. In this case, on average the target generates one measurement per scan, but there could be more. In the ML-PDA case, the number of target measurements per scan is strictly limited to zero or one.)

Table I. ML-PMHT AND ML-PDA PARAMETERS

	ML-PMHT			ML-PDA	
	π_0	π_1	V	λ	P_d
Scen. 1-4	0.95	0.05	1.26×10^9	3.7×10^{-9}	0.8
Scen. 5	0.95	0.05	1.26×10^9	6.7×10^{-10}	0.8
Scen. 1 Rayleigh clut.	0.95	0.05	1.26×10^9	2.0×10^{-7}	0.8

At the conclusion of each scenario, the following metrics were evaluated: target in-track percentage, target position root-mean square error (RMSE), track fragmentation, target duplicate tracks, overall number of false tracks, and average false track length. These metrics were calculated in the following manner. First, tracks were associated with either a target or clutter. A track was associated with a target if its normalized estimation error squared (NEES) value was less than 10 for scenarios with a single target or widely-spaced targets. (In most situations, as is discussed above, the estimators were statistically efficient.) For scenarios with closely-spaced maneuvering targets, the CRLB tended to underestimate the covariance (the estimators were not statistically efficient here), so the NEES was not as reliable in associating tracks to targets. Instead, in these cases, a track was associated with a target if the average distance between track points and their associated truth points was less than 2000 distance units. If a track could be associated with more than one target, then it was assigned to whichever one was closest. Target in-track percentage was then calculated by taking the ratio of target truth points that had a track associated with them to the total number of target truth points. Target duplicate tracks were calculated by simply counting the number of targets that had more than one track associated with them at a given time. The root mean square error was then calculated for all tracks that were associated with targets. This RMSE value was only calculated for a target on points where there was both an ML-PDA track and an ML-PMHT track associated with it. This was done so as not to penalize one algorithm that was barely holding track (with a resultant poor RMSE) while the other algorithm was not tracking at all. Track fragmentation was determined by counting the number of breaks in track for a target. Finally, the overall number of false tracks was simply the number of tracks that were not associated with a target, and the mean false track length was the average number of updates for which a false track was active.

For each of the Monte Carlo sets, 200 runs were performed. Additionally, the confidence intervals shown in Tables II through VIII are at the 95 percent level.

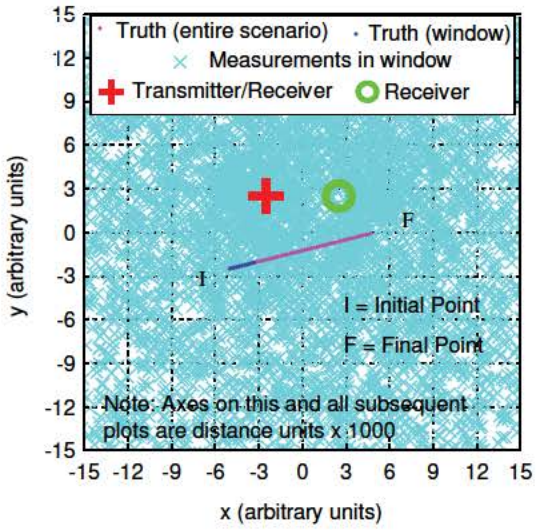

Figure 1. All measurements from a window of data (11 update periods) for scenario 1 with Rayleigh clutter

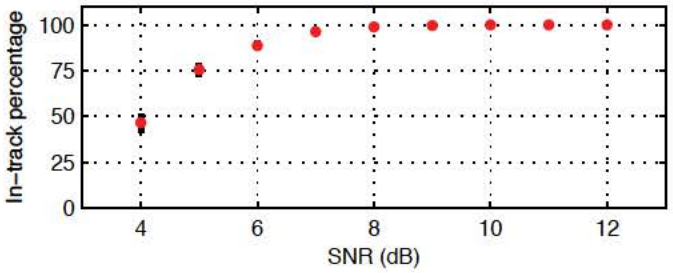

Figure 2. ML-PDA in-track percentage (P_{DT}) vs. expected target SNR for scenario 1 with Rayleigh clutter

III. ML-PDA VS ML-PMHT PERFORMANCE COMPARISONS

Both ML-PDA and ML-PMHT showed themselves to be excellent trackers for targets with low amplitude returns (detailed below). First, to get an idea of the level of difficulty of the problem, all measurements from a batch are plotted in Figure 1 for scenario 1 with the Rayleigh clutter distribution (the scenario with the highest level of clutter).

Using this same scenario, in order to provide a comparison to other algorithms with known performance, in-track percentage as function of SNR was calculated. This is shown in Figure 2 for ML-PDA (results were practically identical for ML-PMHT). For this example (in contrast to the rest of the runs), expected target SNR was fixed, starting at 4 dB with a 2 dB measurement threshold. The expected target SNR was then moved up in 1 dB increments, with Monte Carlo simulations being run at each SNR level. Note that the tracker achieves a P_{DT} of approximately 0.5 at a target SNR of only 4 dB, and a P_{DT} of about 0.9 at 6 dB. By a target SNR of 8 dB, the tracker essentially has a P_{DT} of 1. This shows that ML-PDA and ML-PMHT are very effective very low observable trackers.

After this, ML-PDA and ML-PMHT were run on all five scenarios in their respective multitarget tracking modes. ML-

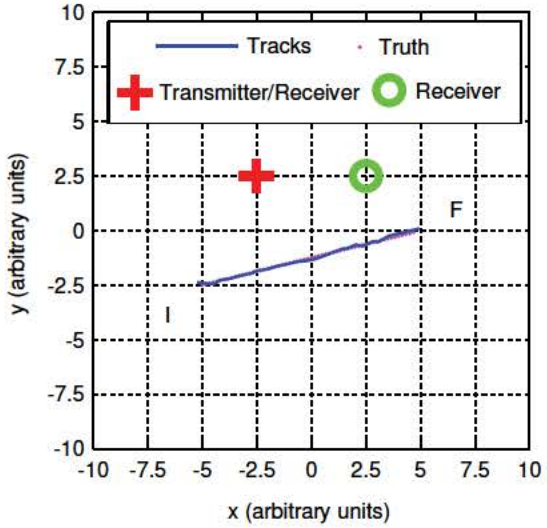

Figure 3. Scenario 1 (baseline) and ML-PDA sample estimated track in one run

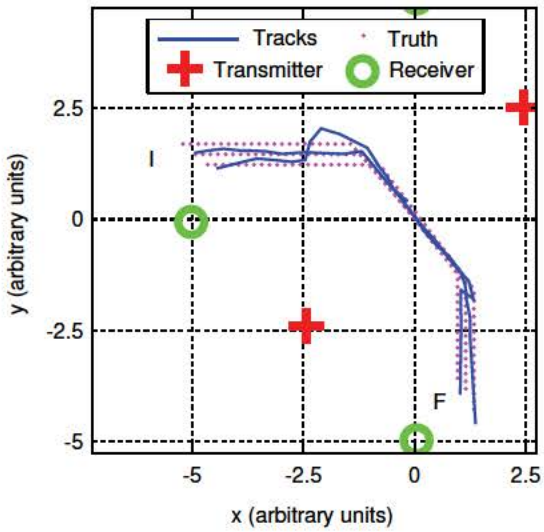

Figure 5. Scenario 2 (three close targets with similar dynamics) and ML-PDA sample estimated tracks in one run

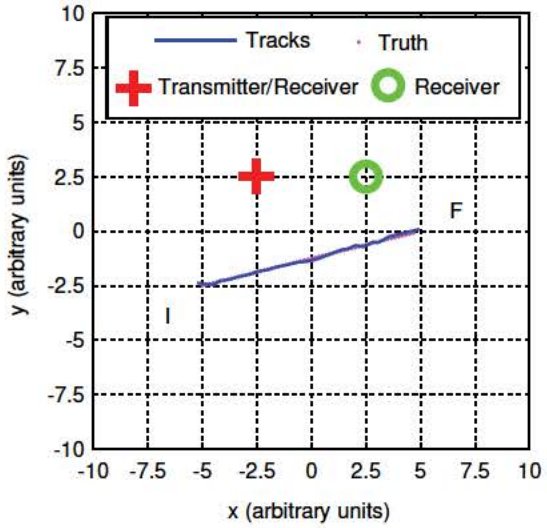

Figure 4. Scenario 1 (baseline) and ML-PMHT sample estimated track in one run

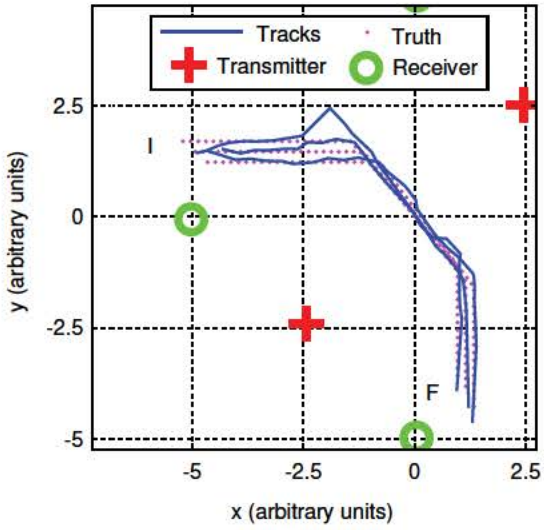

Figure 6. Scenario 2 (three close targets with similar dynamics) and ML-PMHT sample estimated tracks in one run

PDA operated in the sequential single-target mode, while ML-PMHT was run in its true multitarget mode for tracks that were close together.

For scenarios with a single target or easily distinguished targets, ML-PDA and ML-PMHT had virtually identical performance over the Monte Carlo runs. For such target situations, the ML-PMHT log-likelihood ratio should be very close to the ML-PDA log-likelihood ratio, so the tracking results of the two should be similar.

Individual examples taken from the Monte Carlo runs help to illustrate this. For scenario 1, an ML-PDA result shown in Figure 3 and an ML-PMHT result shown in Figure 4 are virtually indistinguishable from each other. For the same scenario with the Rayleigh clutter, results for the two algorithms (Figure 13 for ML-PDA and Figure 14 for ML-PMHT) are also very similar. Finally, for scenario 3, the ML-PDA example in Figure 7 and the ML-PMHT example in Figure 8 appear very much alike.

For the scenarios with targets in close proximity to each other with similar motion dynamics (scenarios 2 and 5), or the scenario with multiple targets that were close enough to potentially cause a tracker to switch targets (scenario 4), the results in Tables II – VII show that ML-PMHT clearly outperforms ML-PDA. This is due to the true multitarget implementation for ML-PMHT in contrast to the sequential single-target tracking logic that is necessary for ML-PDA. In scenario 2, ML-PMHT is able to track targets 1 and 2 in excess of 80 percent of the time and track target 3 nearly 50 percent of the time. In contrast, ML-PDA is tracking target 2 (the middle target) 100 percent of the time, and targets 1 and 3 (the outer targets) less than 10 percent of the time. (Overall, ML-PMHT

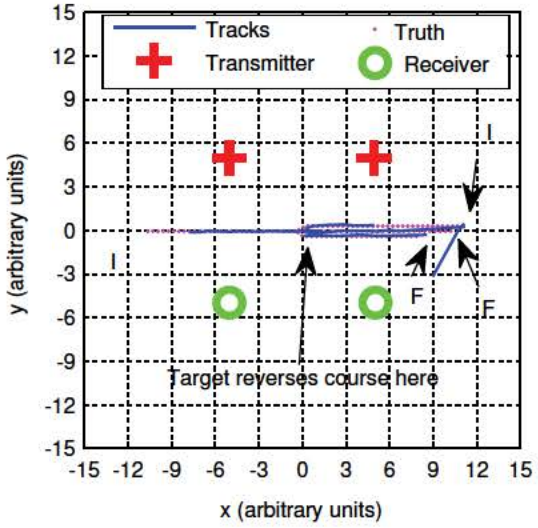

Figure 7. Scenario 3 (two close targets with different dynamics) and ML-PDA sample estimated tracks in one run

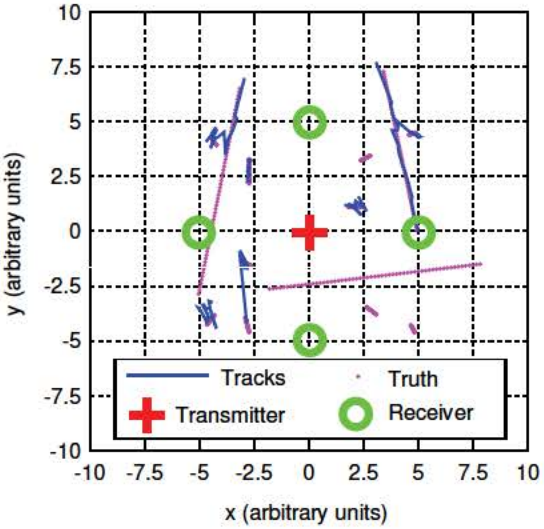

Figure 9. Scenario 4 (large number of targets) and ML-PDA sample estimated tracks in one run

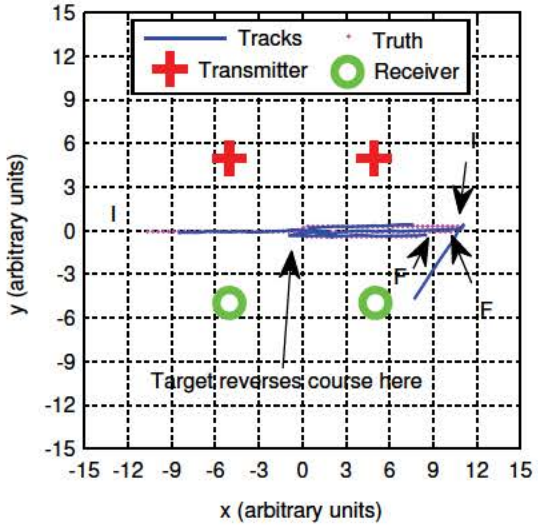

Figure 8. Scenario 3 (two close targets with different dynamics) and ML-PMHT sample estimated tracks in one run

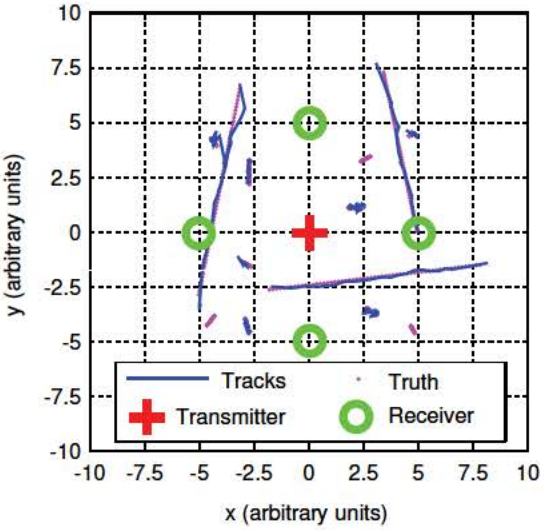

Figure 10. Scenario 4 (large number of targets) and ML-PMHT sample estimated tracks in one run

is tracking at least one target 100 percent of the time.)

The reason ML-PDA is not performing as well as ML-PMHT in this case is the sequential single-target implementation that is necessary for ML-PDA. Figure 15 illustrates what is happening in scenario 2. This figure shows measurements from three targets in close proximity to each other, all moving in the same direction. For clarity of illustration, the measurements have no noise, and there are no clutter measurements shown. ML-PDA is implemented in a sequential mode; the first track "finds" the high-SNR measurement in each scan, and then these measurements are excised from the data. The next track finds the remaining (relatively) high-SNR measurement, and again, these measurements are excised from the data. Since both found tracks are using data from all three true targets, the tracks tend to zigzag back and forth over the middle target (and each other). As a result, the track scoring will most likely result in the middle target being tracked by both tracks. Over many trials, this will produce a high P_{DT} value for the middle target, a duplicate track for the middle target, and low P_{DT} for the outer targets. This is exactly what is seen in the Monte Carlo results for scenario 2 — for ML-PDA the middle target had a P_{DT} of 1, while the outer targets had a P_{DT} of less than 0.1. The middle target also had, on average, 1.07 duplicate tracks associated with it.

In contrast, ML-PMHT, with its more natural and appealing true multitarget formulation, can better find all three targets. Simultaneously optimizing for multiple targets at once prevents the "claiming" of the high-SNR measurement by the first track to run through the data; instead, the high-SNR measurements are more equally (and correctly) divided between the three tracks, as is shown in Figure 16. Scenario 5 showed similar

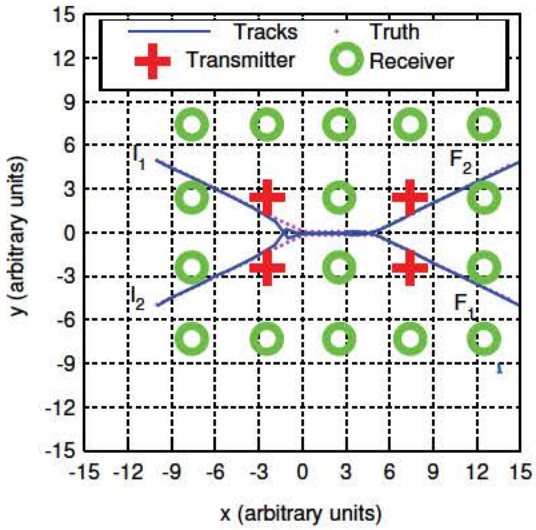

Figure 11. Scenario 5 (switching targets) and ML-PDA sample estimated tracks in one run (switch occurred)

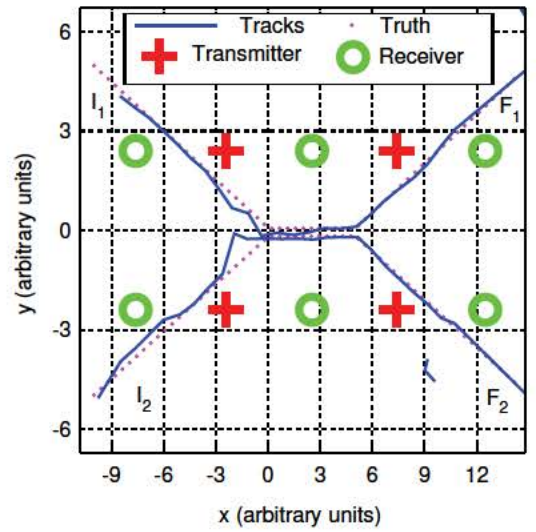

Figure 12. Scenario 5 (switching targets) and ML-PMHT sample estimated tracks in one run, zoomed-in view (no switching occurred)

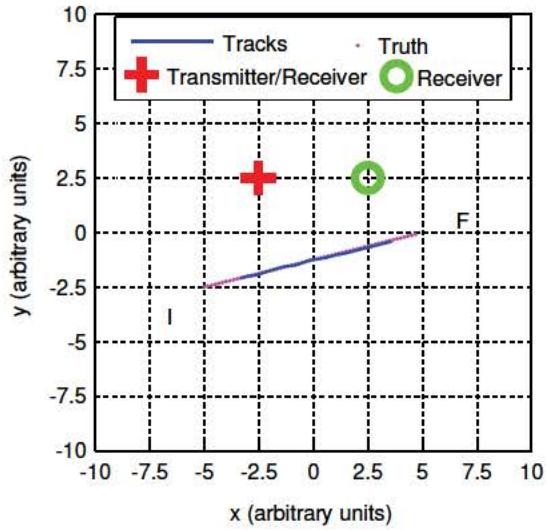

Figure 13. Scenario 1 (baseline) and ML-PDA sample estimated track with high density Rayleigh clutter in one run

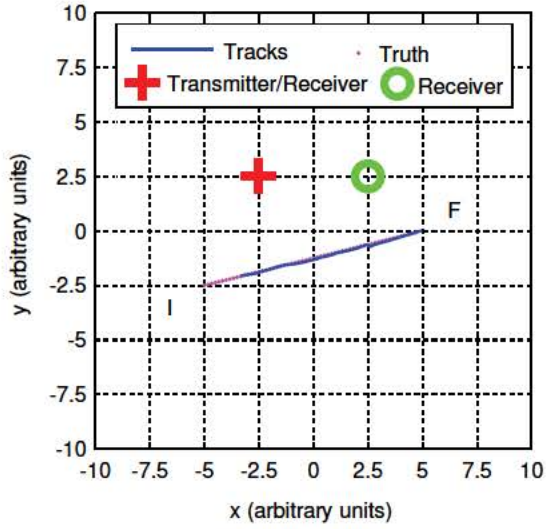

Figure 14. Scenario 1 (baseline) and ML-PMHT sample estimated track with high density Rayleigh clutter in one run

results. ML-PDA was only able to track both targets approximately 45 percent of the time, while ML-PMHT was able to track both targets approximately 65 percent of the time. This number is actually slightly misleading; the relatively low numbers for ML-PDA are due to the fact that tracks using this algorithm switched targets on the portion of the trajectory where the targets were close, and the tracks ended up on the wrong targets, driving down P_{DT}. There was some switching for ML-PMHT as well, but as is seen by the results, ML-PDA was more susceptible to this problem. This is a result of the sequential single-target implementation used for ML-PDA that is described above.

Individual examples from the Monte Carlo runs again reinforce this conclusion. A scenario 2 result for ML-PDA is shown in Figure 5. Here, the first track (on the middle target) "claims" and then excises all the high-SNR measurements. A second track is initiated, and it claims the remaining (relatively) high-SNR measurements, in the process crossing over the first track several times. As a result, it appears that this track would be associated with the middle target as well. There are not enough high-SNR measurements left to form a third track. In contrast, the multitarget ML-PMHT tracker, shown in Figure 6 is able to track all three targets with a minimum of switching. Examples from scenario 5 show similar results. In Figure 11, ML-PDA is not able to separate the targets on the portion of the track where the two targets are paralleling each other at very close range; during this portion, the tracks actually switch between targets five times. In contrast, in Figure 12, the multitarget ML-PMHT tracker is able to track both targets without any switching.

Finally, ML-PMHT outperformed ML-PDA on scenario

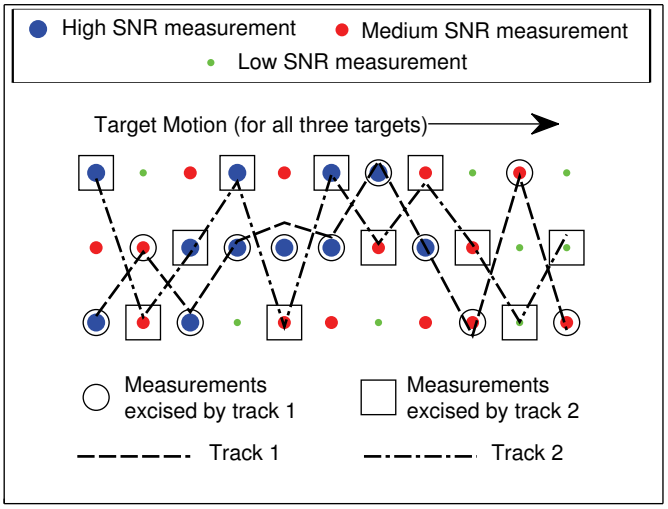

Figure 15. Example of multitrack measurement assignment for ML-PDA

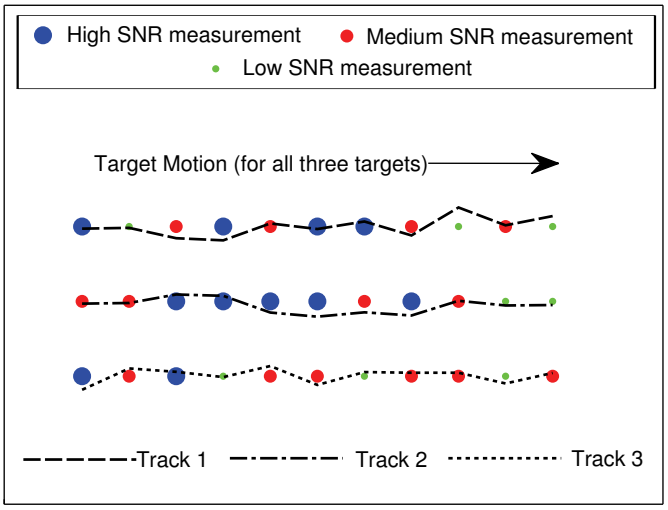

Figure 16. Example of multitrack measurement assignment for ML-PMHT

4 for almost all of the targets for similar reasons. (Results from only targets 7 and 12 are shown below; they are fairly representative of all 13 targets in this scenario). Again, the sequential single target tracking framework for ML-PDA could not perform as well as the true multitarget implementation for ML-PMHT. Tracks using the ML-PDA implementation were far more susceptible to being drawn off from one target to another by high-SNR measurements (similar to the effect illustrated in Figure 15). Compare the performance of ML-PDA on this scenario in Figure 9 with the performance of ML-PMHT in Figure 10. Several instances of track switching are visible in the ML-PDA plot that are not seen in the ML-PMHT plot. While this switching is not between targets with similar dynamics (as happens with Scenarios 2 and 5), it is happening with targets that are moving very slowly. As a result, there are no dynamics — either evolving position over time or Doppler — to differentiate measurements between two targets.

All the simulations up to this point were performed using the ML-PDA target measurement generation model — that

Table II. IN-TRACK PERCENTAGE RESULTS

	ML-PDA		ML-PMHT	
	mean	conf. int. (95 percent)	mean	conf. int. (95 percent)
Scenario 1	95.4	[94.8, 96.0]	95.4	[94.8, 96.0]
Scenario 2 Tgt 1	12.0	[7.5, 16.6]	83.9	[79.6, 88.2]
Scenario 2 Tgt 2	100	[100, 100]	87.5	[83.7, 91.3]
Scenario 2 Tgt 3	1.9	[0.0, 3.8]	53.1	[46.5, 59.7]
Scenario 3 Tgt 1	82.7	[81.0, 84.4]	82.5	[81.0, 84.0]
Scenario 3 Tgt 2	76.1	[74.2, 78.0]	77.1	[75.4, 78.9]
Scenario 4 Tgt 7	61.0	[54.7, 67.4]	91.1	[89.3, 92.8]
Scenario 4 Tgt 12	52.5	[45.9, 59.2]	96.3	[95.9, 96.8]
Scenario 5 Tgt 1	45.3	[38.4, 52.2]	63.1	[56.5, 69.7]
Scenario 5 Tgt 2	48.4	[41.5, 55.4]	63.7	[57.1, 70.2]
Scenario 1 Rayleigh	66.9	[66.0, 67.8]	67.4	[66.6, 68.3]

Table III. RMSE RESULTS

	ML-PDA		ML-PMHT	
	mean	conf. int. (95 percent)	mean	conf. int. (95 percent)
Scenario 1	255.8	[229.7, 281.9]	259.2	[233.0, 285.4]
Scenario 2 Tgt 1	313.4	[257.7, 369.0]	281.4	[267.7, 295.1]
Scenario 2 Tgt 2	247.0	[241.9, 252.1]	280.5	[269.6, 291.5]
Scenario 2 Tgt 3	228.4	[186.7, 270.0]	212.4	[202.3, 222.4]
Scenario 3 Tgt 1	1227.3	[1190.2, 1264.3]	946.6	[904.4, 988.8]
Scenario 3 Tgt 2	799.7	[754.6, 844.8]	878.0	[836.1, 920.0]
Scenario 4 Tgt 7	391.3	[303.8, 478.8]	321.6	[274.5, 377.7]
Scenario 4 Tgt 12	151.6	[124.0, 179.2]	213.2	[177.2, 249.3]
Scenario 5 Tgt 1	213.1	[173.3, 252.8]	244.7	[207.1, 282.2]
Scenario 5 Tgt 2	272.5	[211.3, 333.7]	245.6	[215.2, 276.1]
Scenario 1 Rayleigh	217.6	[191.7, 243.6]	182.4	[166.4, 198.9]

Table IV. FRAGMENTATION RESULTS

	ML-PDA		ML-PMHT	
	mean	conf. int. (95 percent)	mean	conf. int. (95 percent)
Scenario 1	0.01	[0.00, 0.02]	0.01	[0.00, 0.02]
Scenario 2 Tgt 1	0.00	[0.00, 0.00]	0.00	[0.00, 0.00]
Scenario 2 Tgt 2	0.00	[0.00, 0.00]	0.00	[0.00, 0.00]
Scenario 2 Tgt 3	0.00	[0.00, 0.00]	0.00	[0.00, 0.00]
Scenario 3 Tgt 1	0.03	[0.01, 0.06]	0.07	[0.03, 0.10]
Scenario 3 Tgt 2	0.24	[0.17, 0.30]	0.06	[0.02, 0.09]
Scenario 4 Tgt 7	0.00	[0.00, 0.00]	0.00	[0.00, 0.00]
Scenario 4 Tgt 12	0.00	[0.00, 0.00]	0.00	[0.00, 0.00]
Scenario 5 Tgt 1	0.15	[0.07, 0.22]	0.15	[0.09, 0.22]
Scenario 5 Tgt 2	0.09	[0.03, 0.15]	0.15	[0.08, 0.22]
Scenario 1 Rayleigh	0.07	[0.03, 0.10]	0.05	[0.02, 0.08]

Table V. DUPLICATE TRACK RESULTS

	ML-PDA		ML-PMHT	
	mean	conf. int. (95 percent)	mean	conf. int. (95 percent)
Scenario 1	0.18	[0.13, 0.24]	0.02	[0.00, 0.04]
Scenario 2 Tgt 1	0.00	[0.00, 0.00]	0.04	[0.01, 0.08]
Scenario 2 Tgt 2	1.07	[1.01, 1.14]	0.48	[0.39, 0.57]
Scenario 2 Tgt 3	0.00	[0.00, 0.00]	0.00	[0.00, 0.00]
Scenario 3 Tgt 1	0.03	[0.01, 0.06]	0.07	[0.03, 0.10]
Scenario 3 Tgt 2	0.24	[0.17, 0.30]	0.06	[0.02, 0.09]
Scenario 4 Tgt 7	0.00	[0.00, 0.00]	0.09	[0.05, 0.13]
Scenario 4 Tgt 12	0.09	[0.03, 0.14]	0.18	[0.12, 0.24]
Scenario 5 Tgt 1	0.04	[0.00, 0.08]	0.13	[0.07, 0.19]
Scenario 5 Tgt 2	0.02	[0.00, 0.05]	0.11	[0.05, 0.16]
Scenario 1 Rayleigh	2.10	[1.83, 2.37]	0.00	[0.00, 0.00]

Table VI. FALSE TRACK RESULTS

	ML-PDA		ML-PMHT	
	mean	conf. int. (95 percent)	mean	conf. int. (95 percent)
Scenario 1	0.07	[0.03, 0.11]	0.07	[0.03, 0.11]
Scenario 2	0.06	[0.03, 0.09]	0.15	[0.15, 0.21]
Scenario 3	0.34	[0.26, 0.42]	0.26	[0.19, 0.33]
Scenario 4	0.17	[0.10, 0.23]	0.14	[0.09, 0.20]
Scenario 5	2.13	[1.92, 2.34]	2.65	[2.44, 2.86]
Scenario 1 Rayleigh	0.08	[0.02, 0.14]	0.00	[0.00, 0.00]

Table VII. FALSE TRACK LENGTH RESULTS

	ML-PDA		ML-PMHT	
	mean	conf. int. (95 percent)	mean	conf. int. (95 percent)
Scenario 1	3.14	[2.59, 3.69]	3.14	[2.56, 3.73]
Scenario 2	2.75	[2.31, 3.19]	3.37	[2.81, 3.92]
Scenario 3	4.34	[3.18, 5.50]	4.42	[3.32, 5.62]
Scenario 4	6.75	[3.72, 9.78]	11.67	[7.81, 15.52]
Scenario 5	8.98	[7.81, 10.16]	8.55	[7.59, 9.51]
Scenario 1 Rayleigh	3.58	[2.39, 4.78]	0.00	[0.00, 0.00]

is, at most one measurement was generated by the target in any given scan. In this condition, ML-PMHT and ML-PDA had identical performance in the single-target cases, and ML-PMHT outperformed ML-PDA in the small-separation multitarget cases. We now round out the comparison between the two algorithms by considering what happens when the ML-PMHT target measurement generation model is used to generate the data and more than one measurement is allowed to originate from the target (this could happen, for example, in an environment that supported multipath propagation).

In order to do this, Scenario 1 (with K-distributed clutter) was re-run for one, two and three expected target returns per scan. Results for all metrics were virtually the same between the algorithms (and similar to results shown above for Scenario 1), with the exception of the number of duplicate tracks. These results are shown in Table VIII. Here, ML-PDA, as expected, suffers from an increasing number of duplicate tracks as N, the expected number of target measurements per scan, is increased. In contrast, ML-PMHT basically has on average no duplicate tracks for any number of target measurements per scan. With this model of target-measurement generation, ML-PMHT is the superior algorithm.

Table VIII. NUMBER OF DUPLICATE TRACKS AS A FUNCTION OF N, THE EXPECTED NUMBER OF TARGET MEASUREMENTS PER SCAN

	ML-PDA		ML-PMHT	
N	mean	confidence interval (95 percent)	mean	confidence interval (95 percent)
1	1.32	[1.21, 1.43]	0.03	[0.00, 0.05]
2	4.05	[3.88, 4.23]	0.04	[0.01, 0.06]
3	6.12	[5.92, 6.31]	0.09	[0.05, 0.13]

IV. CONCLUSIONS

We developed a true multitarget implementation of ML-PMHT, and compared it to the legacy sequential single-target ML-PDA algorithm with Monte Carlo testing. This testing first showed that ML-PDA and ML-PMHT are effective very low observable (i.e. received target SNR less than 12 dB) trackers, working down to an expected target SNR of 4-5 dB. After this, the ML-PDA and the ML-PMHT tracking algorithms were applied to five different benchmark scenarios with Monte Carlo trials using a target measurement generation model of zero or one measurements originating from the target in a scan. For scenarios with a single target or multiple targets with measurements that could easily be differentiated by dynamics, the performances of ML-PDA and ML-PMHT were identical — ML-PMHT did not suffer from the fact that its measurement assignment model did not match the actual target measurement generation model. In cases with closely-spaced targets with measurements that could not be differentiated easily by dynamics, ML-PMHT outperformed ML-PDA due to the fact that the former had a true multitarget LLR formulation, while the latter had to handle multiple targets in a sequential single-target mode. Finally, when the target measurement generation model was switched to that of ML-PMHT, with multiple measurements per scan being generated by the target, ML-PMHT outperformed ML-PDA in terms of the number of duplicate tracks generated. Overall, the performance of ML-PMHT makes it the preferred algorithm.

REFERENCES

[1] D. Abraham and A. Lyons, "Simulation of non-Rayleigh reverberation and clutter," *IEEE Journal of Oceanic Engineering*, vol. 29, no. 2, pp. 347–362, 2004.

[2] D. Avitzour, "A maximum likelihood approach to data association," *IEEE Trans. on Aerosp. and Electronic Syst.*, vol. 28, no. 2, pp. 560–566, 1996.

[3] Y. Bar-Shalom, X. R. Li, and T. Kirubarajan, *Estimation with Applications to Tracking and Navigation*. John Wiley and Sons, Inc., 2001.

[4] C. Jauffret and Y. Bar-Shalom, "Track formation with bearing and frequency measurements in clutter," *IEEE Transactions on Aerospace and Electronic Systems*, vol. 26, no. 6, pp. 999–1010, 1990.

[5] T. Kirubarajan and Y. Bar-Shalom, "Low observable target motion analysis using amplitude information," *IEEE Trans. on Aerosp. and Electronic Syst.*, vol. 32, no. 4, pp. 1637–1382, 1996.

[6] S. Schoenecker, P. Willett, and Y. Bar-Shalom, "A comparison of the ML-PDA and the ML-PMHT algorithms," in *Proc. of 14th Intern'l Conf. on Info. Fusion*, Chicago, IL, 2011.

[7] ——, "Maximum likelihood probabilistic multi-hypothesis tracker applied to multistatic sonar data sets," in *Proc. SPIE Conf. on Signal Processing, Sensor Fusion, and Target Recognition*, no. 8050-9, Orlando, FL, 2011.

[8] ——, "ML-PDA and ML-PMHT: Comparing multistatic sonar trackers for VLO targets using a new multitarget implementation," *Journal of Oceanic Engineering*, To appear.

[9] R. Streit and T. Luginbuhl, "A probabilisitic multi-hypothesis tracking algorithm without enumeration," in *Proc. 6th Joint Data Fusion Symposium*, Laurel, MD, June 1993.

[10] ——, "Maximum likelihood method for probabilistic multi-hypothesis tracking," in *Proc. SPIE Conf. on Signal and Data Processing of Small Targets*, Orlando, FL, 1994.

[11] ——, "Probabilistic multi-hypothesis tracking," Naval Undersea Warfare Center, Tech. Rep. TR 10428, 1995.